Supplemental Document

applied optics

Ray-tracing model of a perfect lens compliant with Fermat's principle: the Cardinal Lens: supplement

JEFFREY P. WILDE

E. L. Ginzton Laboratory, Stanford University, Stanford, California 94305, USA (jpwilde@stanford.edu)

Supplement DOI: https://doi.org/10.6084/m9.figshare.24969966

Parent Article DOI: https://doi.org/10.1364/AO.507605

Ray-Tracing Model of a Perfect Lens Compliant with Fermat's Principle: The Cardinal Lens: supplemental document

In this supplement, we first include a table that summarizes various use cases for the Cardinal Lens. We then provide additional examples of models in Zemax OpticStudio® [1] that utilize the Cardinal Lens DLL user-defined surface. These models were constructed and tested using OpticStudio version 23.2, but the DLL, which is compiled as a 64-bit DLL, is compatible with older versions of OpticStudio, and even with Zemax Classic. In fact, we find the DLL appears to work properly in Zemax 13 (64-bit version, released June 24, 2015), although very limited testing was done using this older version. Copies of the model files are included in Code 1.

1. CARDINAL LENS CONFIGURATIONS: SUMMARY TABLE

The following table illustrates various Cardinal Lens configurations. The user is required to enter values for the lens effective focal length (EFL) and its optimal paraxial magnification (m_p). The local object and image (i.e., left and right) conjugate plane distances, z_1 and z_2, respectively, are measured with respect to the first and second principal planes of the lens. For numerical purposes, $|m_p| \leq$ 1e-10 corresponds to infinite front conjugate while $|m_p| \geq$ 1e+10 corresponds to infinite rear conjugate. The values for z_1, z_2 and m_p should be consistent with the lens equation as shown in Eq. 6 of the main paper.

Lens Configuration	Layout	EFL	m_p (Paraxial Mag.)	z_1 (left conjugate)	z_2 (right conjugate)
Positive Imaging Lens - finite conjugate - real object / real image	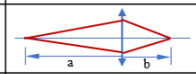	$+f$	$-\lvert b/a \rvert$ (n_1/n_2)	$-\lvert a \rvert$	$+\lvert b \rvert$
Positive Imaging Lens - finite conjugate - real object / virtual image	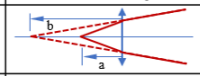	$+f$	$\lvert b/a \rvert$ (n_1/n_2)	$-\lvert a \rvert$	$-\lvert b \rvert$
Negative Imaging Lens - finite conjugate - real object / virtual image	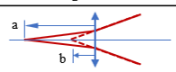	$-f$	$\lvert b/a \rvert$ (n_1/n_2)	$-\lvert a \rvert$	$-\lvert b \rvert$
Negative Imaging Lens - finite conjugate - virtual object / virtual image	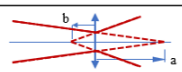	$-f$	$-\lvert b/a \rvert$ (n_1/n_2)	$+\lvert a \rvert$	$-\lvert b \rvert$
Positive Focusing Lens - infinite front conjugate	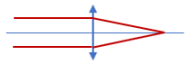	$+f$	$\lvert m_p \rvert \leq$ 1e-10	±1e10	$+n_2 f$
Positive Collimation Lens - infinite rear conjugate	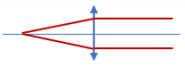	$+f$	$\lvert m_p \rvert \geq$ 1e+10	$-n_1 f$	±1e10
Negative Diverging Lens - infinite front conjugate	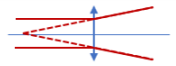	$-f$	$\lvert m_p \rvert \leq$ 1e-10	±1e10	$-n_2 f$
Negative Collimation Lens - infinite rear conjugate	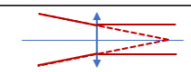	$-f$	$\lvert m_p \rvert \geq$ 1e+10	$+n_1 f$	±1e10

Table S1. Table of common configurations in which the Cardinal Lens may be used.

2. ADDITIONAL CARDINAL LENS MODEL EXAMPLES

A. Negative Cardinal Lens for Virtual Imaging

In this case, we use a negative Cardinal Lens to generate virtual images of two field points (NA = 0.1) that are telecentric in object space. The lens has a focal length $f = -10$ mm and a thickness of 2 mm. The transverse magnification is 0.50. Figure S1 shows a layout on the left in

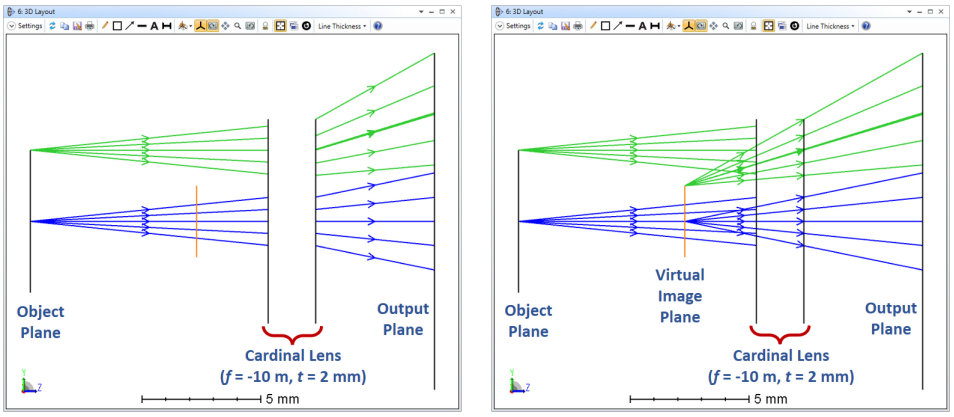

Fig. S1. Example of a negative Cardinal Lens ($f = -10$ mm) with a thickness of 2 mm creating virtual images of two telecentric field points. Rays propagating to the virtual image plane are not drawn in the layout on the left, but they are shown on the right.

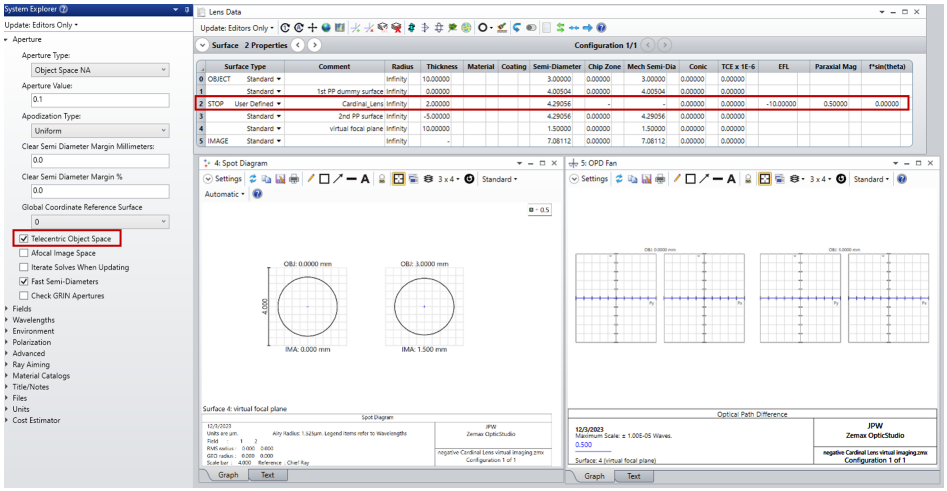

Fig. S2. Screenshot of the OpticStudio model window showing the sequence of surfaces along with spot diagram and OPD fan analysis windows which clearly show perfect imaging.

which only forward propagating rays are displayed, while the layout on the right shows rays backpropagating to the virtual image plane. Figure S2 is a screenshot from OpticStudio that shows the sequence of surfaces in the Lens Data Editor. Negative thickness backpropagation allows rays to propagate from the second principal plane of the lens to the virtual image surface. This screenshot also demonstrates perfect imaging with spot diagrams displaying point-focus images and zero OPD across the entrance pupil for the two fields, both analysis windows being set for evaluation at the virtual image plane surface.

B. Mirror-Space Example

The Cardinal Lens may be used in mirror space (i.e., following reflection by a mirror surface). Figure S3 shows two paraxial lenses with a mirror in between them to relay the object plane to an intermediate focal plane in mirror space. A Cardinal Lens with a thickness of 5 mm then re-images the intermediate focal plane with m_p = -0.5 into a space with a refractive index of 1.5.

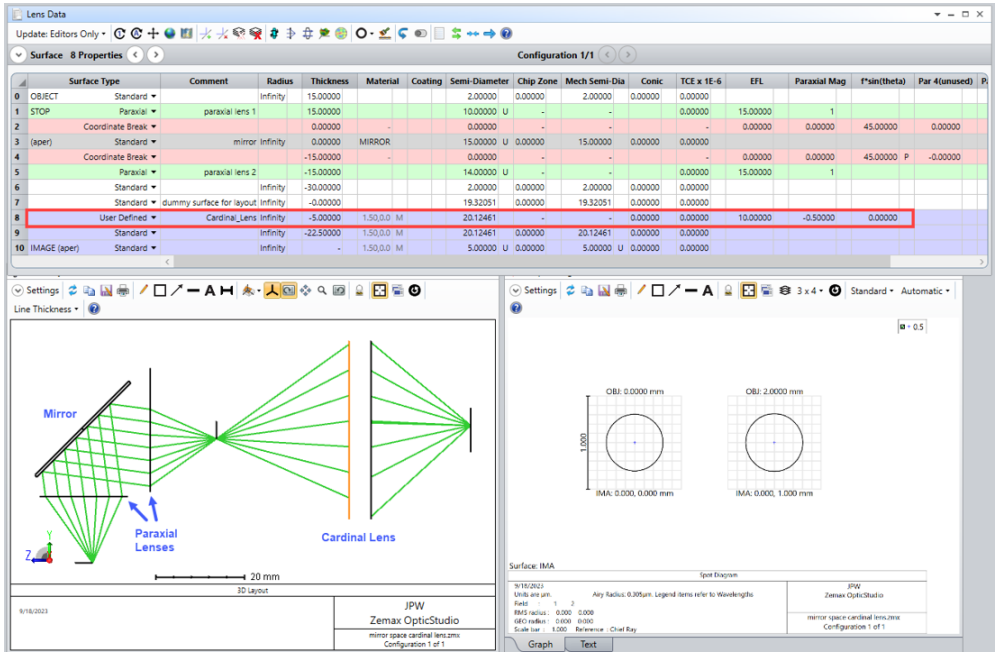

Fig. S3. Example of the Cardinal Lens used in mirror space to relay an intermediate focal plane. The lens thickness, like other thicknesses in mirror space, is negative; in this case it is -5 mm.

C. System Stop on Cardinal Lens 2nd Principal Plane

All of the examples in the main body of the paper have the system stop either in front of or on the 1st principal plane of the initial Cardinal lens in the optical path – so ray aiming is not needed. However, if the stop is placed on or after the 2nd principal plane of the Cardinal lens, then paraxial ray should be utilized. The stop size may need to be chosen by using an iterative approach in which it is initially set to a small value and incrementally increased until either the desired value is reached or the ray aiming algorithm fails to work across the entire stop. The pupil compress values may also need to be incrementally increased during this process

An example is illustrated in Figs. S4-S6. It is a finite-conjugate imaging arrangement with a paraxial magnification m_p = -0.25. The Cardinal lens has a thickness of 10 mm and an EFL equal to 10 mm. Two field points are shown with y-coordinates of 0 and 5 mm. The input and output

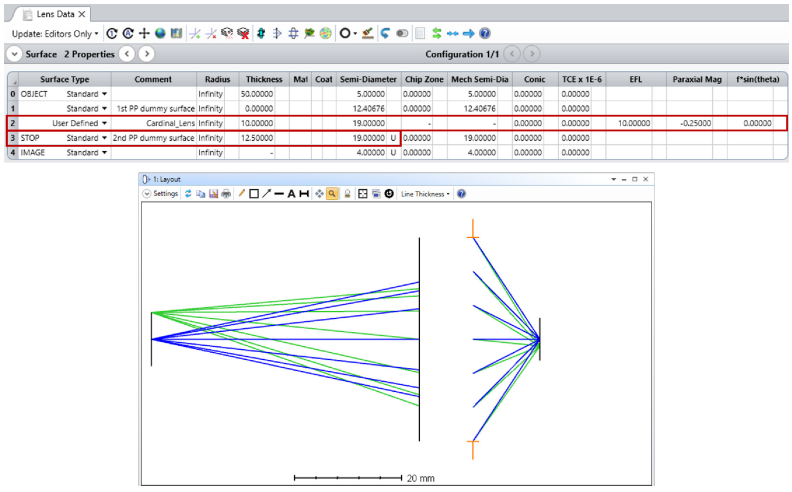

Fig. S4. Cardinal Lens used in a finite-conjugate imaging layout with the system stop placed on the 2nd principal plane of the lens. Paraxial ray aiming is required.

numerical apertures are 0.21 and 0.83, respectively. As seen in Fig. S5, the system aperture is designated as "float by stop size" so that the stop radius is set by the clear semi-diameter on the 2nd principal plane surface. Uniform filling, or apodization, of the stop is chosen. Paraxial ray aiming is turned on and the stop radius is incrementally increased until reaching a value of 19 mm; however, a pupil compress factor of 0.9 for both x and y (i.e., a 90% compression of the paraxial entrance pupil size) is needed to ensure convergence of the ray aiming algorithm. To confirm proper ray aiming, the user can look at the pupil aberration fans, which should display small values across the entire pupil, or monitor the ray footprint diagram on the stop surface, which should show rays distributed across the full stop area with a distribution given by the chosen form of aperture apodization (see Fig. S6). If the ray aiming fails, then the pupil aberration fans are not plotted and the text data shows NaN values at one or more pupil locations. For the example here, the ray aiming fails when trying to further increase the stop size or use a smaller pupil compression factor.

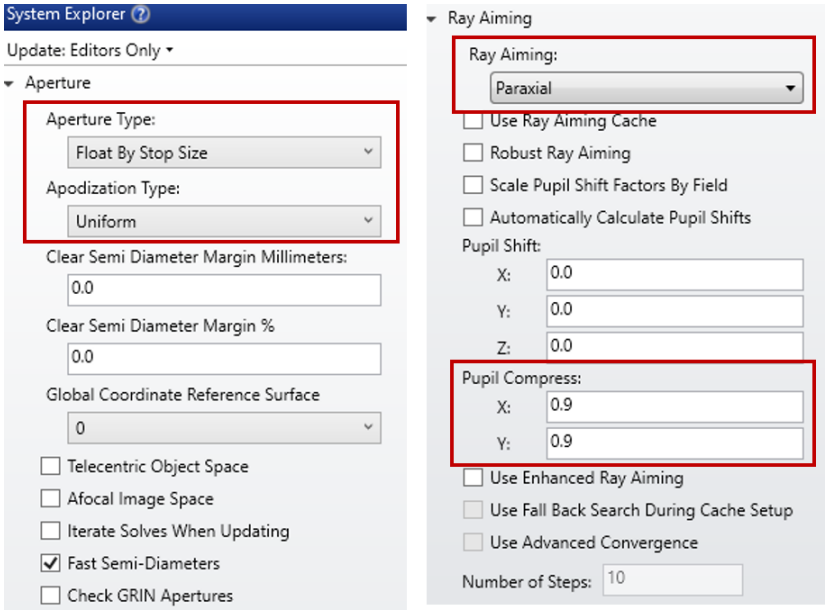

Fig. S5. Aperture and ray aiming settings used for the layout shown in Fig. S4.

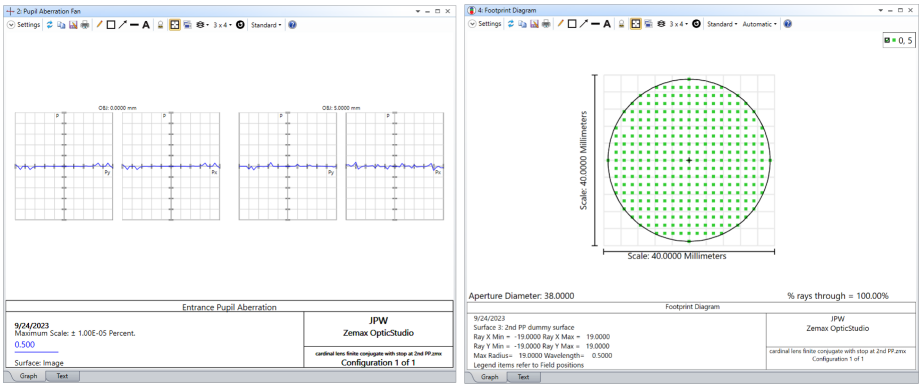

Fig. S6. Pupil aberration plots and ray footprint diagram in the stop plane (which is the 2nd principal plane of the Cardinal lens). These results demonstrate that the ray aiming algorithm for the layout shown in Fig. S4 is working properly.

D. Spherical Aberration for a Cardinal Lens used at Non-Optimal Magnification

In the main body of the paper (Sec. 5.5) we provide an example of the aberrations introduced when the Cardinal Lens is not used at its specified optimal magnification. Here we provide one more example in which the spherical aberration is directly compared to analytical results derived from an eikonal formulation as described by Walther ([2], Sec. 31.2).

Consider a 40X microscope objective in air with an EFL = 4 mm and NA = 0.85, used with the object plane 10 μm closer to the lens than it should be, yielding an operating magnification of -44.44. The layout is shown below in Fig. S7. The stop is placed in the back focal plane and paraxial ray aiming is turned on. Rays leaving the on-axis object point have direction cosines (L, M). Figure S8 shows a plot of the transverse spherical aberration versus L from our model (with $M = 0$); data points from the Walther reference ([2], Table 31.1) are overlaid for comparison. We find that our model agrees precisely with the analytical results.

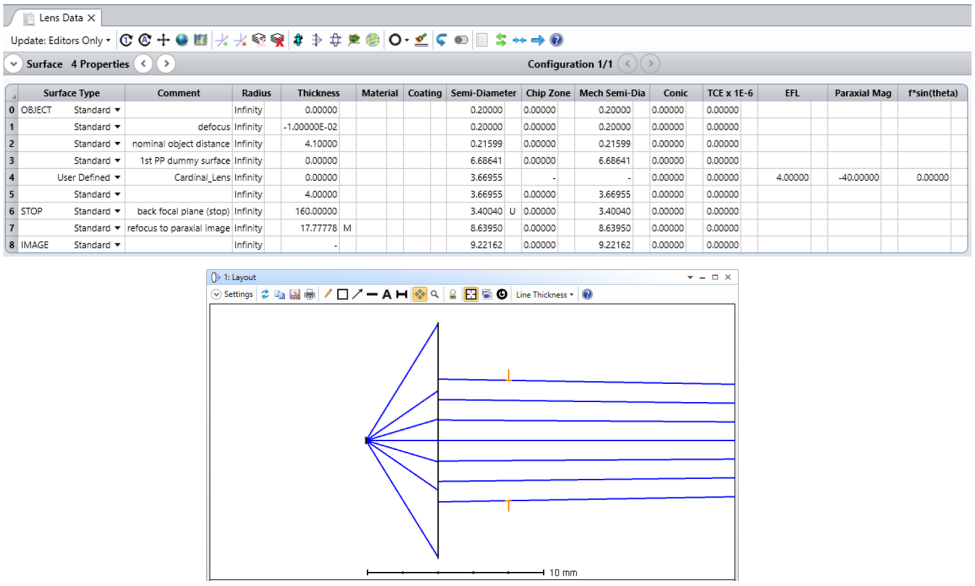

	Surface Type		Comment	Radius	Thickness	Material	Coating	Semi-Diameter	Chip Zone	Mech Semi-Dia	Conic	TCE x 1E-6	EFL	Paraxial Mag	f*sin(theta)
0	OBJECT	Standard		Infinity	0.00000			0.20000	0.00000	0.20000	0.00000	0.00000			
1		Standard	defocus	Infinity	-1.00000E-02			0.20000	0.00000	0.20000	0.00000	0.00000			
2		Standard	nominal object distance	Infinity	4.10000			0.21599	0.00000	0.21599	0.00000	0.00000			
3		Standard	1st PP dummy surface	Infinity	0.00000			6.68641	0.00000	6.68641	0.00000	0.00000			
4		User Defined	Cardinal_Lens	Infinity	0.00000			3.66955		-	0.00000	0.00000	4.00000	-40.00000	0.00000
5		Standard		Infinity	4.00000			3.66955	0.00000	3.66955	0.00000	0.00000			
6	STOP	Standard	back focal plane (stop)	Infinity	160.00000			3.40040	U 0.00000	3.40040	0.00000	0.00000			
7		Standard	refocus to paraxial image	Infinity	17.77778	M		8.63950	0.00000	8.63950	0.00000	0.00000			
8	IMAGE	Standard		Infinity	-			9.22162	0.00000	9.22162	0.00000	0.00000			

Fig. S7. A Cardinal lens simulates a 40X microscope objective operating at a magnification of -44.44 which introduces spherical aberration. The object-space NA = 0.85.

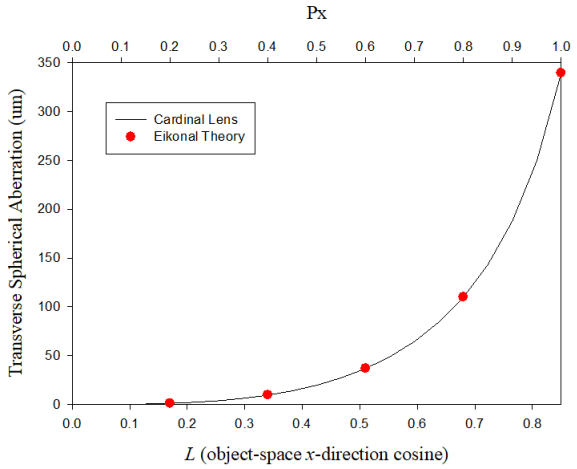

Fig. S8. Transverse spherical aberration plotted as a function of L (the x-direction cosine of an object-space ray). The results from the Cardinal lens model are compared to analytical data points found using eikonal function theory ([2], Table 31.1).

E. Grating Imaging

A nice example of the difference between a paraxial lens and a Cardinal Fourier transform (FT) lens is provided by grating imaging based on a two-lens telecentric coherent imaging system. In this case an amplitude grating with a frequency of 200 cycles/mm is located in the front focal plane of the first imaging lens (f_1 = 10 mm) and is illuminated by a monochromatic plane wave (λ = 0.50 μm). A second lens (f_2 = 2 mm) is used to construct the grating image by placing it a distance of $f_1 + f_2$ from the first imaging lens. The system therefore has a magnification of $m = f_2/f_1 = 0.2$.

The amplitude grating is mathematically taken to have the following form: $t(x,y) = \cos(2\pi f_g y)$ where $f_g = 200$ mm^{-1} is the grating frequency. This object has two Fourier components, namely the ± 1 diffraction orders. Taking into account the magnification, the "perfect" image intensity is

$$I(x,y) = \left| t\left(\frac{x}{m}, \frac{y}{m}\right)\right|^2 = \cos^2(2\pi f_g y/m) = \frac{1}{2}\left[\cos\left(4\pi f_g y/m\right) + 1\right]. \tag{S1}$$

We see the grating image should be periodic with frequency $2f_g/m = 2(200)/0.2 = 2{,}000$ mm^{-1} (i.e., the grating image should have a period of 0.50 μm).

We begin by constructing the system using paraxial lens as shown in Fig. S9. Two configurations are used, one for each of the two diffraction orders. To generate the coherent image, we use the Huygens PSF analysis tool with both configurations contributing so that we observe the coherent sum of the two diffraction orders when they arrive at the image plane (Fig. S10). As expected,

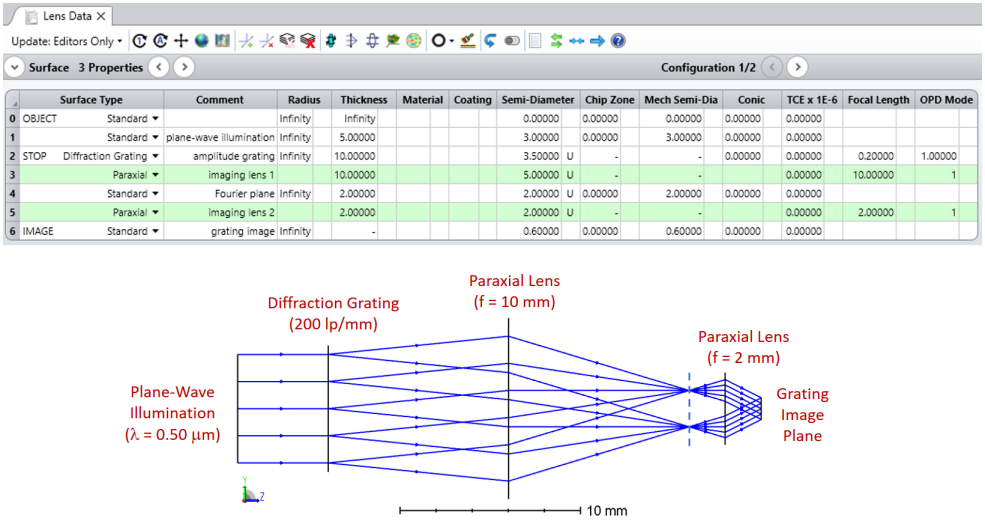

Fig. S9. Imaging of a sinusoidal amplitude grating with a pair of paraxial lenses.

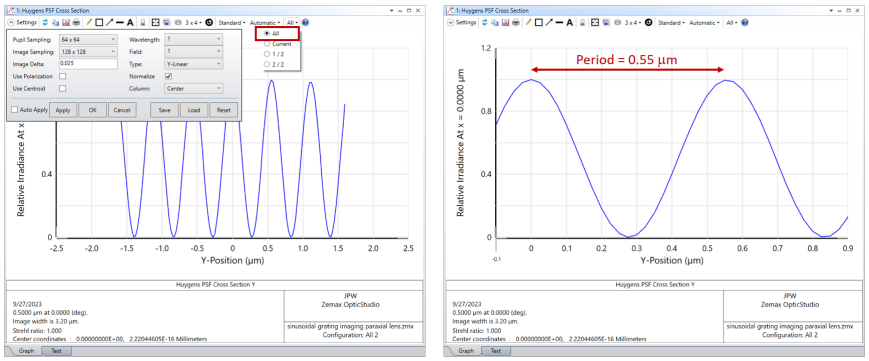

Fig. S10. Cross-section of the grating image irradiance formed with paraxial lenses. The period is not consistent with the transverse magnification.

the image is sinusoidal, but upon closer inspection we see the period is 0.55 μm, not the ideal value of 0.50 μm. This error is a consequence of the fact that the paraxial lenses do not provide the necessary $f\sin(\theta)$ mapping, characteristic of a Fourier transform lens.

We can modify the layout by using Cardinal lenses operating in FT mode as illustrated in Fig. S11. As before, we utilize the Huygens PSF analysis to generate the grating image, but in

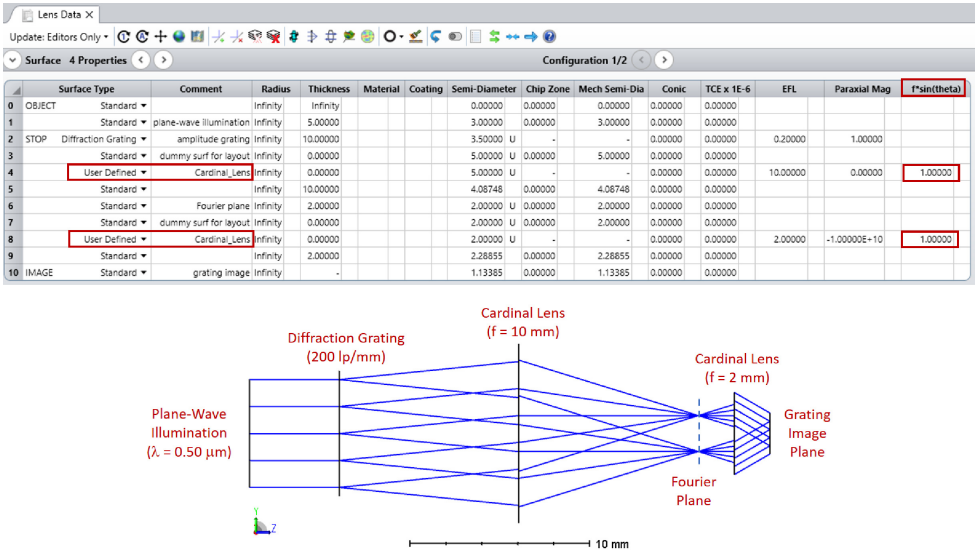

Fig. S11. Imaging of a sinusoidal amplitude grating with a pair of Cardinal lenses operating in Fourier transform mode with $f\sin(\theta)$ distortion.

this instance the image fringe can display a lateral shift, or phase offset, because the chief rays for the two diffraction orders do not in general intersect the image plane at the origin and instead have offset intercept points as shown in Fig. S12. Of course, in practice, any lateral shift of the grating itself would produce a corresponding shift of its image, so this effect is not particularly important. However, if desired, we can eliminate the fringe shift in the model and thereby center the fringe image without too much difficulty. To do this we need to impart a relative phase shift between the two diffraction orders. To main symmetry, we choose to phase advance one beam and phase delay the other. As indicated in Fig. S12, the required wavefront phase adjustment for a given chief-ray intercept offset is simply given by $\phi = \delta/\lambda = y_c M/\lambda$. Here y_c is the y-intercept coordinate of the chief ray at the image plane, and M is the chief ray y-direction cosine. The

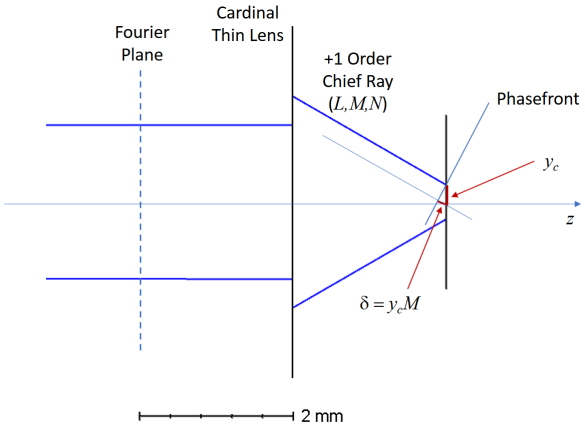

Fig. S12. Diagram showing how to calculate the phase offset needed to center the grating image. Here δ is the path length offset, which is converted to phase upon dividing by the wavelength.

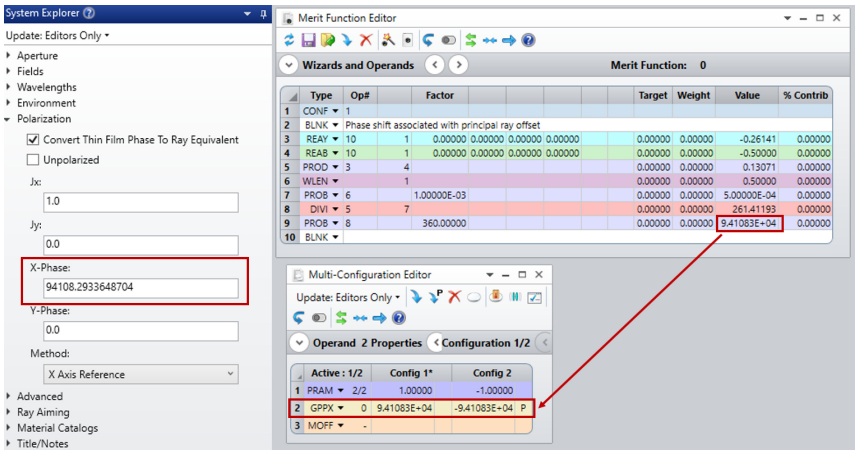

Fig. S13. The proper phase shift adjustment is calculated in the merit function editor and applied with opposite signs to the two diffraction orders to center the grating image.

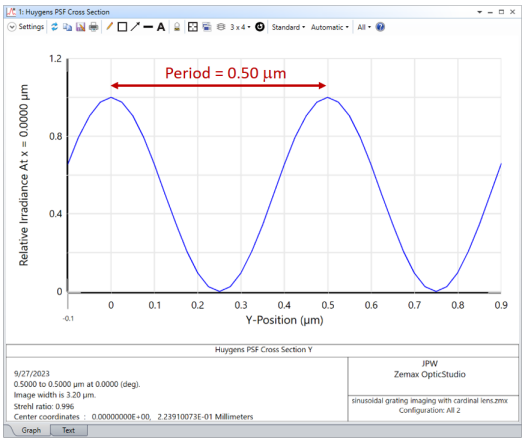

Fig. S14. Cross-section of the grating image irradiance formed with Cardinal lenses operating in Fourier-transform mode. The period is consistent with the transverse magnification.

phase offset ϕ can therefore be easily calculated in the merit function and then applied, with the appropriate sign, to a given diffraction order via the polarization settings as shown in Fig. S13. During propagation OpticStudio applies a clockwise phasor rotation to the field, so the overall phase becomes increasingly negative as the ray propagates. Consequently, advancing the phase requires adding a negative phase offset, while delaying the phase corresponds to a positive offset. Doing this by the proper amount centers the fringe image on the origin. Now, with that detail having been addressed, we see in Fig. S14 the image fringe pattern formed by the Cardinal lenses has the correct period because the lenses have the proper $f\sin(\theta)$ distortion.

F. Zoom Lens and Conversion of a Paraxial Lens to a Cardinal Lens

The design of a zoom lens often begins with two or more paraxial lenses having variable separations in order to provide a tunable effective focal length, thereby allowing a user to zoom in or out when imaging a distant object. Once the paraxial version is constructed with the desired first-order properties, the lens designer must then replace each paraxial lens with an equivalent lens group made from glass elements. In this example, we will take the opposite approach, beginning with an actual zoom lens design (provided as a sample with OpticStudio) and subsequently converting it first to paraxial form, then finally replacing the paraxial lenses with Cardinal lenses. To facilitate this last step a macro is provided that calculates the conjugate distances and magnification for a paraxial lens embedded in the optical train.

We begin with the zoom lens sample file provided with OpticStudio [3]. It is a two-group

design (positive-negative) taken from US Patent 4936661. Figure S15 shows the layout for three separate zoom configurations. Using the EFLX merit function operand, we can easily find the

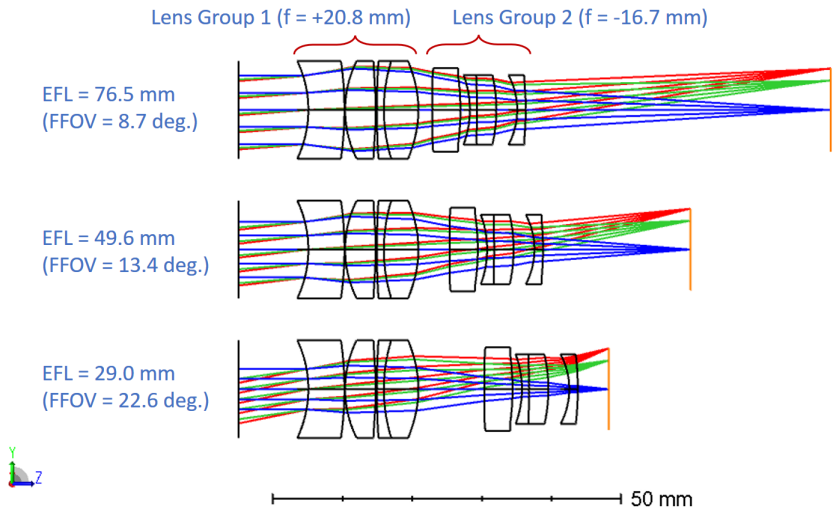

Fig. S15. Zoom lens sample file provided with OpticStudio.

focal lengths of the two lens groups, and then replace them with paraxial lens versions. For each configuration, the separation between the two paraxial lenses, as well as the distance from the second lens to the image plane, are found via optimization with a merit function that drives the paraxial version to have the same EFL as the actual zoom lens. The paraxial lens layout is shown in Fig. S16.

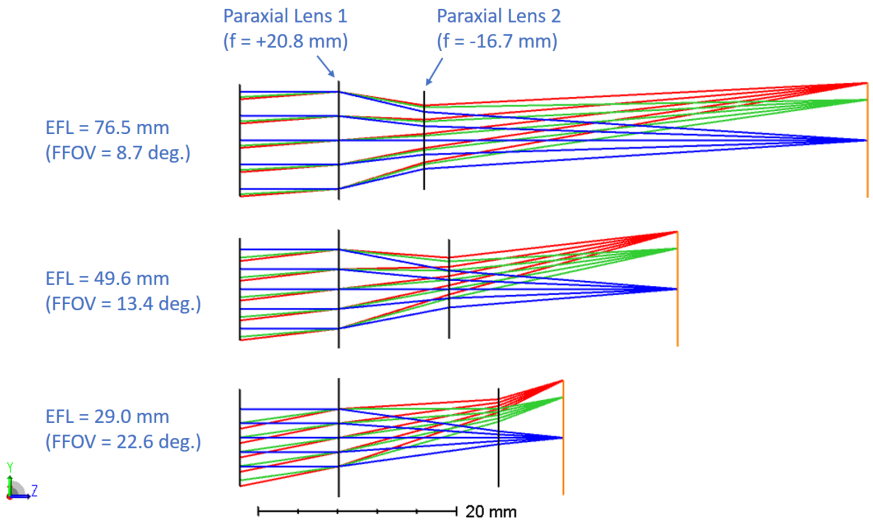

Fig. S16. Paraxial lens version of the zoom system shown in Fig. S15.

We now turn our attention to replacing the paraxial lenses with Cardinal lenses. Doing so will illustrate the details associated with this transition (specifically how to choose the appropriate magnification for Cardinal lens) along with the pros and cons of using Cardinal lenses in this application. The first paraxial lens is used in an infinite-front-conjugate configuration, so the paraxial magnification is zero and conversion to a Cardinal lens is trivial. However, the second paraxial lens is used in a finite-conjugate arrangement. Moreover, the magnification at which it is used varies as the zoom is adjusted. Because a Cardinal lens is designed to work optimally

only at a single magnification, we must pick one of the configurations to replicate. Here we select the middle one (Config 2). Then naturally the question arises, what is the magnification value at which the second paraxial lens operates in Config 2? It is not obvious from a simple visual inspection of the layout, but a simple macro can be used to provide the answer.

We provide a macro (ZPL65.zpl) that can be used in conjunction with the ZPLM merit function operand to return the conjugate distances and paraxial magnification for any paraxial lens in the layout. The surface number of the paraxial lens of interest is entered into the "Hx" cell. In our case Paraxial Lens 2 resides at surface 2. For "Data" values of 0, 1, and 2, the macro returns the front conjugate distance, the rear conjugate distance, and the paraxial magnification, respectively. Figure S17 a screen shot showing how the Lens 2 magnification changes from one configuration to the next. To make the conversion to Cardinal lenses, we select Pmag = 2.38 from Config 2. The resulting layout and spot diagram matrix are shown in Fig. S18. Config 2 remains diffraction

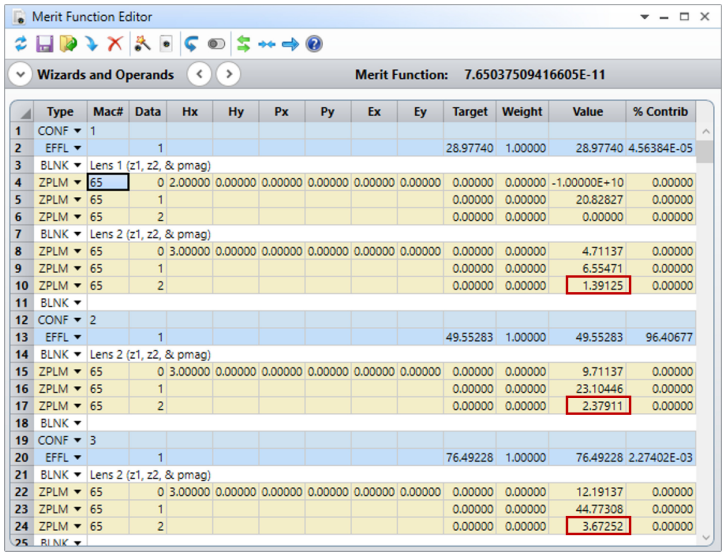

	Type	Mac#	Data	Hx	Hy	Px	Py	Ex	Ey	Target	Weight	Value	% Contrib
1	CONF	1											
2	EFFL		1							28.97740	1.00000	28.97740	4.56384E-05
3	BLNK	Lens 1 (z1, z2, & pmag)											
4	ZPLM	65	0	2.00000	0.00000	0.00000	0.00000	0.00000	0.00000	0.00000	0.00000	-1.00000E+10	0.00000
5	ZPLM	65	1							0.00000	0.00000	20.82827	0.00000
6	ZPLM	65	2							0.00000	0.00000	0.00000	0.00000
7	BLNK	Lens 2 (z1, z2, & pmag)											
8	ZPLM	65	0	3.00000	0.00000	0.00000	0.00000	0.00000	0.00000	0.00000	0.00000	4.71137	0.00000
9	ZPLM	65	1							0.00000	0.00000	6.55471	0.00000
10	ZPLM	65	2							0.00000	0.00000	1.39125	0.00000
11	BLNK												
12	CONF	2											
13	EFFL		1							49.55283	1.00000	49.55283	96.40677
14	BLNK	Lens 2 (z1, z2, & pmag)											
15	ZPLM	65	0	3.00000	0.00000	0.00000	0.00000	0.00000	0.00000	0.00000	0.00000	9.71137	0.00000
16	ZPLM	65	1							0.00000	0.00000	23.10446	0.00000
17	ZPLM	65	2							0.00000	0.00000	2.37911	0.00000
18	BLNK												
19	CONF	3											
20	EFFL		1							76.49228	1.00000	76.49228	2.27402E-03
21	BLNK	Lens 2 (z1, z2, & pmag)											
22	ZPLM	65	0	3.00000	0.00000	0.00000	0.00000	0.00000	0.00000	0.00000	0.00000	12.19137	0.00000
23	ZPLM	65	1							0.00000	0.00000	44.77308	0.00000
24	ZPLM	65	2							0.00000	0.00000	3.67252	0.00000
25	BLNK												

Fig. S17. Example of using the provided macro (ZPL65.zpl) to determine what the magnification values are for the second paraxial lens in the three configurations of the zoom layout of Fig. S16.

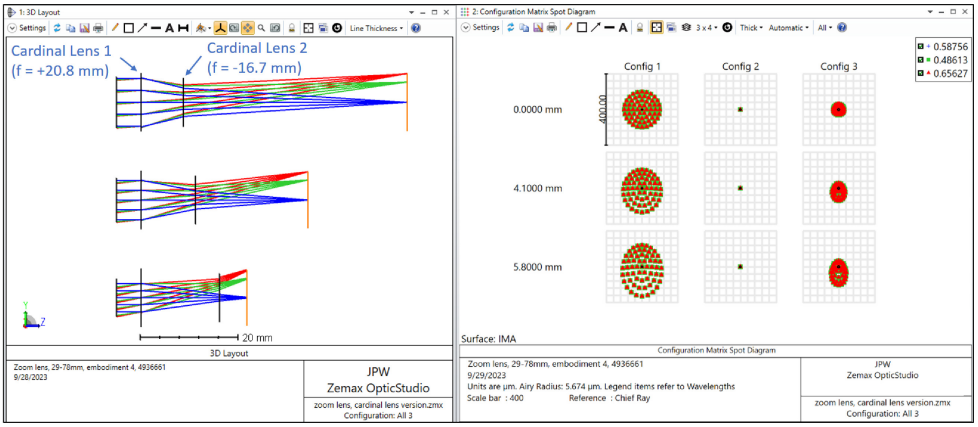

Fig. S18. Cardinal lens version of the zoom system shown in Fig. S15. The magnification of the second cardinal lens is chosen for optimal performance in the middle of the zoom range (Config 2).

limited, while Config 1 and Config 3 incur aberration. This is to be expected since Cardinal Lens 2

is only optimized for Config 2. Therefore, Config 2 remains aberration-free, while Config 1 and Config 3 incur aberration.

In turn, this result suggests that if a lens or lens group needs to work well over a range of finite conjugate conditions, then it should not be designed to obey the sine condition for a fixed magnification. In this zoom lens example, the two lens groups can be designed such that there is some degree of aberration balancing across the zoom range. In general, the extent to which an actual lens deviates from the sine condition can be quantified by the "Offense against the Sine Condition" (OSC) value; for example, see the OSCD merit function operand.

REFERENCES

1. Zemax OpticStudio,® Ansys Inc., Canonsburg, PA, USA (https://www.ansys.com).
2. A. Walther, *The Ray and Wave Theory of Lenses* (Cambridge University Press, 1995).
3. See, for example: "`C:\Users\Username\Documents\Zemax\Samples\Sequential\Zoom_systems\Zoom_lens.zmx`." Here "Username" should be replaced by the appropriate user account name, and the underscores represent white spaces.